

PAPER • OPEN ACCESS

## Assessment of AA7075/SiO<sub>2</sub> surface composites fabricated by friction stir processing (FSP)

To cite this article: M. H. Abd El-Aziz *et al* 2019 *IOP Conf. Ser.: Mater. Sci. Eng.* **610** 012022

View the [article online](#) for updates and enhancements.



**ECS** **240th ECS Meeting**  
Digital Meeting, Oct 10-14, 2021  
**We are going fully digital!**  
Attendees register for free!  
**REGISTER NOW**

## Assessment of AA7075/ SiO<sub>2</sub> surface composites fabricated by friction stir processing (FSP)

M. H. Abd El-Aziz <sup>1,2</sup>, A.B. El-Shabasy <sup>3</sup>, M. M. Z. Ahmed <sup>4,5</sup> and H. A. Hassan <sup>3</sup>

<sup>1</sup> MSc, Department of Design and Production Engineering, Ain Shams University, 1 Elsarayat St., Abbaseya, Cairo 11517, Egypt

<sup>2</sup> Plant design Engineer, Power Generation and Engineering Services Company, 41 El Salam Avenue, 5th settlement, New Cairo, Cairo, Egypt.

<sup>3</sup> Professor, Department of Design and Production Engineering, Ain Shams University, 1 Elsarayat St., Abbaseya, Cairo 11517, Egypt.

<sup>4</sup> Associate Professor, Mechanical Engineering Department, The British University in Egypt, Al-Sherouk 11837, Cairo, Egypt

<sup>5</sup> Associate Professor, Metallurgical and Materials Engineering Department, Faculty of Petroleum and Mining Engineering, Suez University, 43721 Suez, Egypt.

E-mail: [mohamedhazem.meca@gmail.com](mailto:mohamedhazem.meca@gmail.com)

**Abstract.** Friction stir processing (FSP) was developed based on the same principles of friction stir welding (FSW) mainly to enhance the surface properties of various materials and to produce surface composites. In this work surface composites of AA7075 as the metal matrix that reinforced with ultra-fine sized SiO<sub>2</sub> particles were developed using FSP. A groove of 3 mm depth and 1.2 mm width was made on the surface of AA7075 to provide the highest reinforcement volume fraction on the produced surface composites. FSP tool with a square profiled tool pin of 3.5 mm pin length and of 5mm pin side was used. The FSP parameters used were 600 rpm and 50 mm/min. The developed surface composites were evaluated using different metallographic techniques to investigate the macro and micro features. Also the hardness profile was measured across the processed zone. The surface composites achieved by three consecutive passes of processing showed uniform particle distribution across the stirring zone of the surface composite. Moreover, the surface composite hardness was improved by 10-30% compared to the unreinforced alloy. The tool with a square profiled tool pin enables obtaining sound surface without any visible defects.

### 1. Introduction

Friction Stir Processing (FSP) is a solid-state process used to modify surface of materials in terms of microstructure mainly by grain refinement and development of metal matrix composites (MMCs). FSP was derived from Friction Stir Welding (FSW). In FSW/FSP a non-consumable rotating tool, consisting of a shoulder and a pin, is plunged into two abutting or monolithic sections resulting in the heating and softening of the surrounding material. This leads to localized severe plastic flow about the rotating tool, i.e. stirring, which produces the joint without melting. The aim of this work is to produce surface metal matrix composite using FSP technique.

The tool profile is one of the essential parameters in FSP. Tool shoulders are designed to frictionally heat the surface regions of the workpiece [1]. Tool pin outer profile which is the responsible feature for material stirring was studied in a number of works [2, 3, 4, 5, 6]. The influences of tool pin profile on



the mechanical and metallurgical properties of results FSW/ FSP zone were investigated [7]. Vijay et al. [4] reported that using tapered pin result in narrower stirring zone and coarser grains than when using tool pin with straight profile.

The proper tool material for friction stir processing used for different workpiece materials and reinforced powder was studied previously [1]. It was reported that no significant wear was found on the steel tool when used with Al sheets [1]. The squared profile pin with concave shoulder was used in this work.

## 2. Experimental work

The base metal used for the present work was AA7075 -T6 aluminium alloy plate with 25 mm thickness. SiO<sub>2</sub> powder with particle size range 0.5 - 5 µm was used as reinforcement. Particle size measurement was carried out using scanning electron microscope (SEM).

The tool profile selected for the present work is square profiled pin tool. Shoulder diameter of 20 mm with a concave feature of 6 degrees was used as recommended by previous works [2, 4]. The ratio between the shoulder diameter and pin size was 3 to control heat input as reported by Mishra et al [1]. The pin has diagonal of 7 mm and 3.5 mm length. Pin bottom is tapered by 10 degrees to enable defect free stirring zone [6]. The detailed tool features are shown in Figure 1. The square profile was formed by spark die forming to ensure low stress at the corners, sharp feature edges and accurate dimensions. The tool was made of K110 and heat treated to both HRC 45 and 60. The taper bottom, figure 1, decreases forces during penetration. The concave shoulder used to accumulate more material between tool and pass surface and to apply more pressure during stirring. This shape could enhance the microstructure properties through refining reinforcement powder grain size.

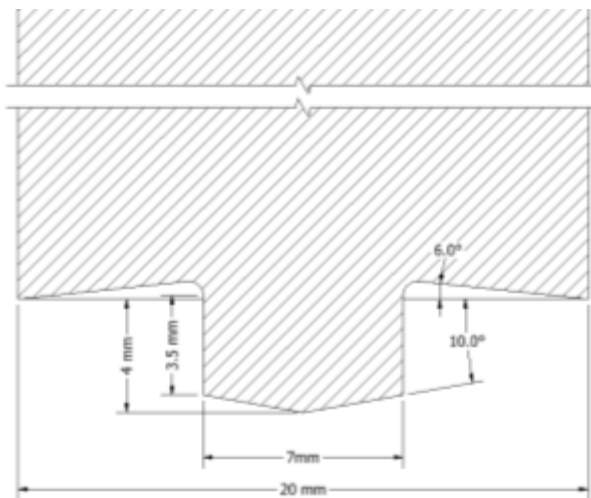


**Figure 1.** Tool with square pin profile



**Figure 2.** Friction stir welding machine spindle

The maximum groove depth was smaller than the pin length to enhance the tool pressing during processing. In addition, decreasing the defects possibility [8]. Groove depth will be 3 mm at least a groove width of 1.2 mm is required. Based on that the groove dimensions were 3 mm length and 1 mm width. The FSP specimens were carried out using friction welding machine at the friction stir welding and processing laboratory at Suez University was used to produce friction stir processed specimens. Before stirring the powder into the matrix a flat pin less tool is used to close the surface of the groove to trap the powder inside the groove. A single path is done in the total length of groove using the pin less tool with rotational speed of 800 rpm in clock wise direction and 50 mm/min feed rate. Axial force

of spindle was from 900 to 1180 kg. By the end of this path the powder is enclosed in the groove. Then the tool changed to the square pin tool. The stirring passes were carried out at rotational speed of 600 rpm clock wise, plunging (vertical) feed of 3 mm/min. and longitudinal feed rate of 50 mm/min. In all cases the plunging speed stopped when the successful axial force of 900 kg was reached. Three consecutive passes were performed using the same tool to ensure good distribution of powder inside the stirring zone.

The machine spindle is tilted 3 degrees during processing. An inclination angle of the tool from 1 to 3 degree is essential. Tilting is essential to increase stirring zone integrity because of the higher hydrostatic pressure applied by the back of the shoulder and promote material flow [9, 10].

Specimens selected for hardness measurements, macro and micro examination were taken from different positions starting from 15 mm after tool indentation center point.

Specimen surface was ground using 2400-grit SiC paper and was polished to a mirror finish using diamond paste. The Specimens were prepared for macrostructure examination after polishing by etching with Keller's reagent according to The ASM Metals Handbook [11] to clarify the macrostructure. SEM with an operating voltage of 20 kV was used to examine the structure of the produced surface composites as well as measuring the reinforcement particle size.

Vickers microhardness indentations were obtained using a microhardness machine with a diamond Vickers indenter, 1 kg indentation load, and an indentation time of 15 seconds. The hardness was measured in two directions At least five indents were made on both sides around the stirring zone centerline. Five indents were made also across the depth of surface composites.

### 3. Results and discussion

The produced AA7075/SiO<sub>2</sub> surface composites were examined visually. Figure 3 shows a defect free surface with good surface finish with no flash along the specimen. Similar results obtained through the specimen cross section whereas no tunnels observed. Figure 4 shows macrographs of material flow in the stirring zone of AA7075/SiO<sub>2</sub> after etching. The advanced side of the tool where a tangent to the rotation in the direction of rotation is the same direction as the traverse direction [12] and it is on the left side in figure 4. The side of the tool where a tangent to the rotation in the direction of rotation is in the opposite direction to the traverse direction this side is called "retreating side" and it is on the right side in figure 4.

Grain size variation between stirring zone and thermomechanical affect zone (TAZ) is shown in figure 5. Reinforcement particles refine the grains inside the stirring zone during recrystallization. While recrystallization in the TAZ led to coarse grain structure. The advanced side of the stirring zone got a clear sharp change in grain size between the stirring zone and heat affected zone, figure 5. In addition, no defects were observed in the side in contrary with previous works which considered the advanced side a preferable zone for defects. On the other hand, the transition in the retreating side is more gradual consistent with work by Nandan et al. [12] while, particles aggregation traces were observed near retreating side surface. This can be attributed to material flow from advanced side to retreating side during FSP. Despite using square profiled tool with good stirring properties and performing three passes of processing to distribute the powder. Onion rings appeared on the stirring zone, Figure 4, can be attributed to the square tool. This tool geometry leads to great pressure variation on the pressure of material behind the tool creating different grain size zones [13].

The ultra-fine grains observed inside the stirring zone of AA7075/SiO<sub>2</sub> surface composite, Figure 5, caused by the square profile tool. Generally second phase particles hinder the material movement during stirring [14]. This tool geometry leads to second phase fragmentation and redistribution especially in case of high strength aluminum alloys [14, 15]. El-Rayes et al. [16] achieved similar results on AA6082-T651.

Figure 10 shows micro bands of ultra-fine SiO<sub>2</sub> particles in the stirring zone. This observation is consistent with Sharma et al work [15]. Although, Sharma et al. [15] reported areas depleted from particles among these bands, this was not recorded in the current work. The micro bands formation can

be attributed to the presence of ultra-fine size of  $\text{SiO}_2$  and the second phase particles exist in AA7075 Al-alloy, moreover, it is alloy dependent [17].



**Figure 3** FSP pass with no flash and smooth surface finish



**Figure 4** Macrograph of FSP stirring zone etched by Keller reagent

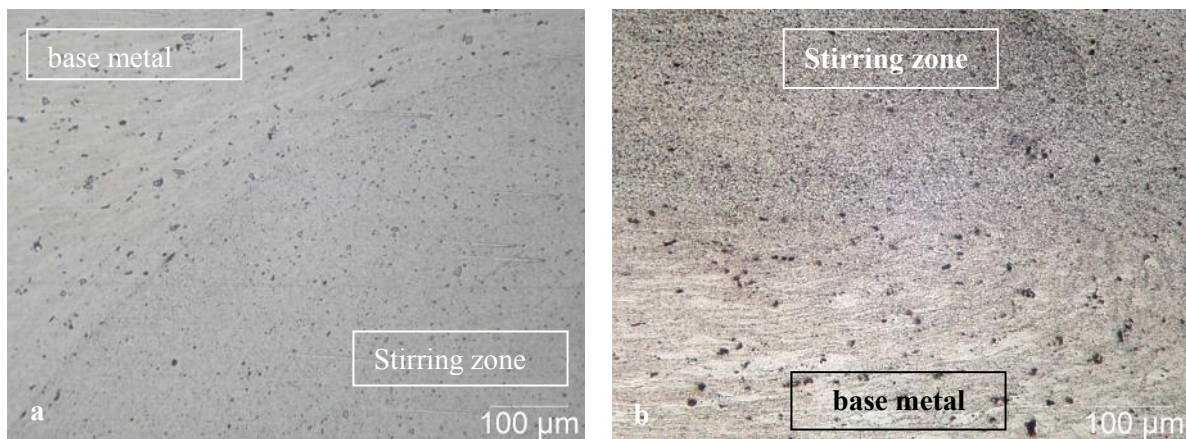


**Figure 5** Metallography of the FSPed zone a) advanced side b) retreating side

Surface composites produced by three passes showed almost uniform particles distribution. Increasing the number of passes increases efficiency of powder mixing with base alloy as well as increases the powder volume fraction in agreement with previous works [16, 18].

SEM micrographs showed uniform  $\text{SiO}_2$  particle distribution in the stirring zones between the micro bands. More examination was carried out on stirring zone structure to recognize the different phases in the AA7075-matrix. Energy-dispersive X-ray (EDX) was used to conduct this analysis, figure 6. It was found that particles of reinforcement on the polished surface was detached from the material leaving surface voids. Silicon oxide is easily found on the chemical analysis of these voids however particles

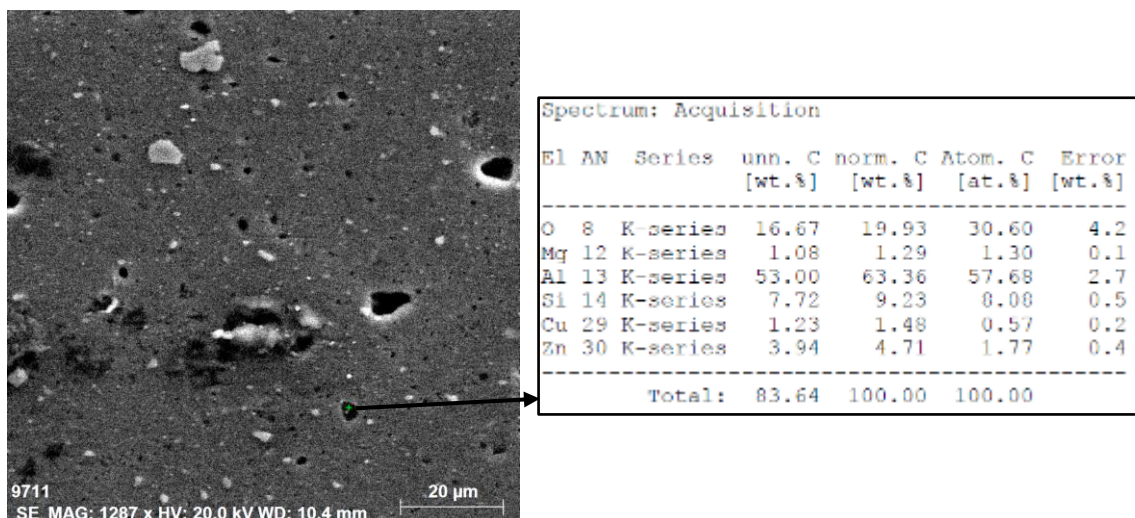


are not visible. This analysis presented a high concentration of silicon and oxygen elements than the standard material maximum limit was found in the surface voids.

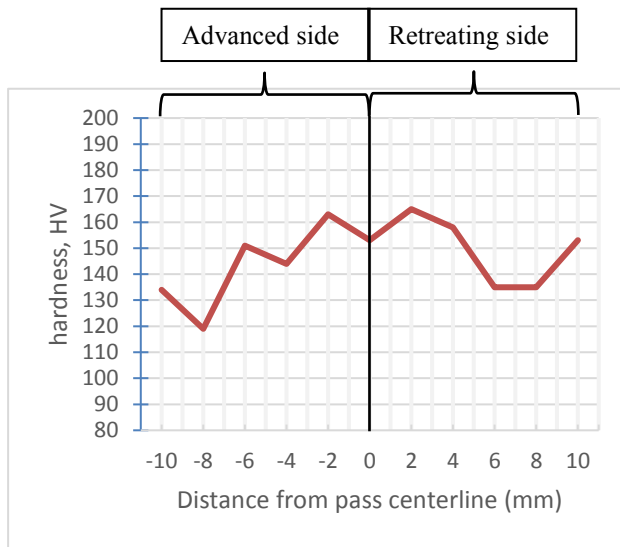
The microhardness values of AA7075/SiO<sub>2</sub> composites are significantly affected by the particle volume fraction and the location of measurements. The highest hardness value was obtained at the composite surface, figure 8 . Increasing the measuring distance from the surface decreased the hardness due to reduction in reinforcement volume fraction. Hardness measurement values on the retreating side are higher than advanced side due to the extrusion action of material from the advanced side to the retreating side. Hardness measurements from stirring zone to TAZ drops sharply in the advanced side and gradually in the retreating side due to the grain size transition difference as mentioned before. The hardness values drops close to the end of the stirring zone and rises again in HAZ. The difference between expansion factors of base metal and reinforced zone resulted in high stress in the HAZ leading to high hardness values than base metal. The average microhardness of the base metal was 120 HV. Conducting FSP on the AA7075 T6 resulting in reducing the hardness of the processed zone due to the softening process resulting from generated heat by FSP. While addition of ultra-fine grained ceramic oxide as reinforcement by FSP resulted in increasing the hardness of the processed zone than the base metal. Figure 7 show an increase in hardness values in processed area by 10 to 30% compared to base metal. Micro defects found during the analysis like reinforcement clusters formed on the retreating side or the micro bands had no effect on the microhardness values through the specimen.

Figure 9 shows material deposition on the edges of square pin tool which change the tool geometry to round and decrease its advantage in better powder distribution and powder particle break down (particle size reduction). However this deposition had no significant effect on the processed composites consistent with Rai et al. work [19].

The tool hardness played a great role in the presently and in many previous works. The K110 tool with HRC60 was not successful in the current work as the tool broke when the machine spindle was tilted. This disagrees with Rai et al. [19] work on AA6062/Al<sub>2</sub>O<sub>3</sub> using threaded tool profile. The source of tool fracture is concave shape of the shoulder and the tool tilting angle. The tilting angle as well as concave shape resulted in high stresses exerted on the tool and led to its brittle fracture. The tool with HRC 45 was successful in agreement with Mishra et al [1]. The tool with HRC 45 is recommended to avoid tool fracture especially with high strength aluminium alloys [5].



**Figure 6** EDX analysis of FSP AA7075 /SiO<sub>2</sub> surface composite



**Figure 7** Hardness Measurement across stirring zone

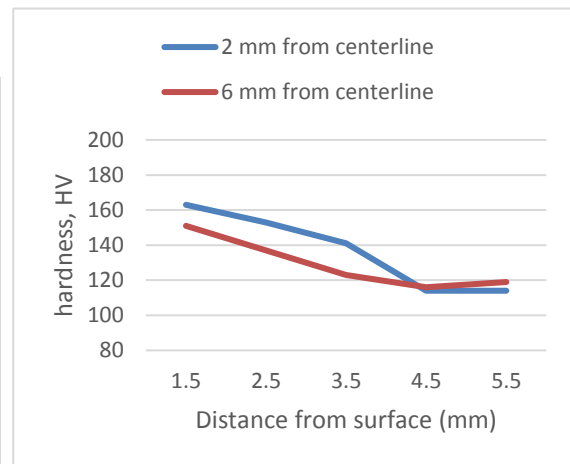


**Figure 8** Hardness Measurement from surface to bottom



**Figure 9** Aluminum deposition on square shape pin

#### 4. Conclusions

The FSP tool design and process parameters used in this work were chosen based on the previous researches and preliminary experiments. A square profiled tool pin produced surface composite from AA7075 plate and SiO<sub>2</sub> particles free of defects. The surface composites achieved by three consecutive passes of processing showed uniform particle distribution across the stirring zone of the surface composite. Hardness properties was enhanced by refining the grains and by addition of ceramic reinforcement. Moreover, the surface composite hardness was improved by 10-30% compared to the unreinforced alloy. Tool wear was negligible and material deposition on square profile pin have no significant effect on the processed surface composite properties.

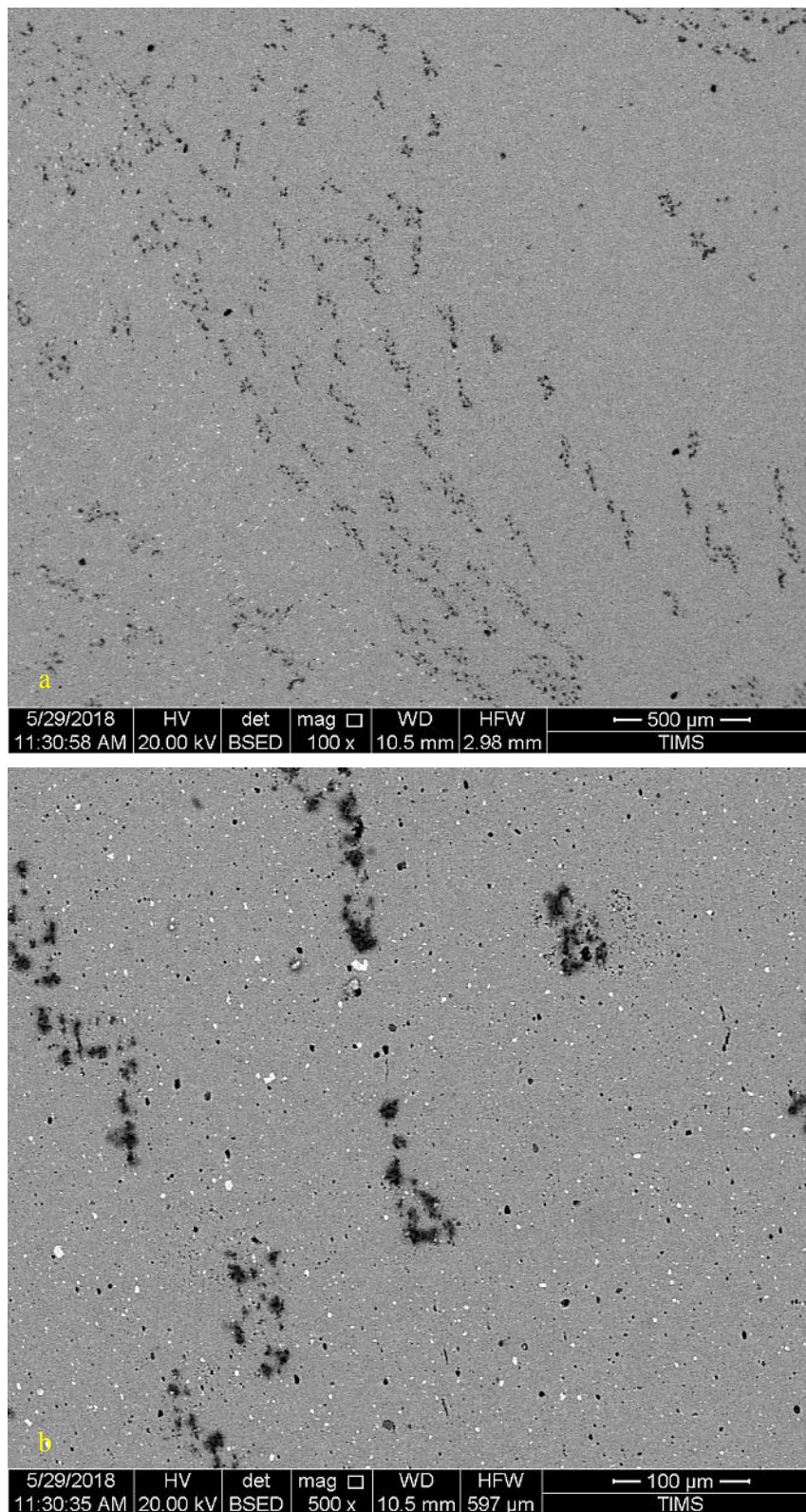


**Figure 10** SEM micrographs of powder distribution patterns

a) bands formation of reinforcement silicon oxide

b) magnification on microbands show ultra-fine sized silicon oxide powder distributed around



## References

- [1] R. S. Mishra and P. S. D. N. Kumar, *Friction Stir Welding and Processing*, Springer, 2015.
- [2] K. Elangovan, V. Balasubramanian and M. Valliappan, "Influences of tool pin profile and axial force on the formation of friction stir processing zone in AA6061 aluminium alloy," *International Journal for Advanced Manufacturing Technology*, vol. 38, p. 285–295, 2007.
- [3] G. Padmanaban and V. Balasubramanian, "Selection of FSW tool pin profile, shoulder diameter and material for joining AZ31B magnesium alloy-An experimental approach," *Material Design*, vol. 30, p. 2647–2656, 2009.
- [4] S. Vijay and N. Murugan, "Influence of tool pin profile on the metallurgical and mechanical properties of friction stir welded Al–10 wt-% TiB<sub>2</sub> metal matrix composite," *Material and Design*, vol. 31, p. 3585–3589, 2010.
- [5] S. Rajakumar, C. Muralidharan b and V. Balasubramanian, "Influence of friction stir welding process and tool parameters on strength properties of AA7075-T6 aluminium alloy joints," *Materials and Design*, 2010.
- [6] D. VENKATESWARLU, N. R. MANDAL, M. M. MAHAPATRA and S. P. HARSH, "Tool Design Effects for FSW of AA7039," *Welding Journal*, vol. 92, pp. 41-47, 2013.
- [7] R. Palanivel, P. K. Mathews and N. Murugan, "Influences of tool pin profile on the mechanical and metallurgical properties of friction stir welding of dissimilar aluminum alloys," *Int. Journal of Engg. Science and Technology*, vol. 2, no. 6, p. 2109–2115., 2010.
- [8] A. THANGARASU, N. MURUGAN, I. DINAHARAN and S. J. VIJAY, "Microstructure and microhardness of AA1050/TiC surface composite fabricated using friction stir processing," *Sadhana*, vol. 37, no. 5, p. 579–586, 2012.
- [9] M. A. Sutton, A. P. Reynolds, B. Yang and R. Taylor, "Mode I fracture and microstructure for 2024-T3 friction stir welds', Mater.," *Material Science Engineering A*, vol. A354, pp. 6-16, 2003.
- [10] J. Lumsden, , "G. Pollock and M. Mahoney: 'Effect of tool design on stress corrosion resistance of FSW AA7050-T7 451 in 'Friction stir welding and processing III," TMS, San Francisco, CA, 2005.
- [11] "Metallography and Microstructure," in *ASM Metals Handbook*, vol. 9, ASM International, 2004.
- [12] R. Nandan, T. Debroy and H. Bhadeshia, "Recent advances in friction-stir welding-Process, weldment structure and properties," *Prog. Material Science*, vol. 53, p. 980–1023, 2008.
- [13] P. L. Threadgill, A. J. Leonard, H. R. Shercliff and P. J. Withers, "Friction stir welding of aluminium alloys," *International Materials Reviews*, vol. 54, no. 2, pp. 49-93, 2009.
- [14] W. J. Arbegast, "A flow-partitioned deformation zone model for defect formation during friction stir welding," *Scripta Material*, vol. 58, p. 372–376, 2008.
- [15] V. Sharma, U. Prakash and B. V. Manoj Kumar, "Surface composites by friction stir processing: A review," *Journal of Materials Processing Technology*, no. 224, pp. 117-134, 2015.
- [16] M. M. El-Rayes and E. A. El-Danafa, "The influence of multi-pass friction stir processing on the microstructural and mechanical properties of Aluminum Alloy 6082," *Journal of Materials Processing Technology*, vol. 212, p. 1157–1168, 2012.
- [17] M. W. Mahoney, C. G. Rhodes, j. G. Flintoff, R. A. Spurling and W. H. Bingel, "Distribution of tensile property and microstructure in friction stir weld of 6063 aluminum," *Metall. Mater. Trans.*, vol. 29A, pp. 1955-1964, 1998.
- [18] D. M. Rodrigues, A. Loureiro, C. Leitao, R. M. Leal and B. Chaparro, "Influence of friction stir welding parameters on the microstructural and mechanical properties of AA 6016-T4 thin welds. 30 (6),," *Materials and Design*, vol. 30, no. 6, p. 1913–1921, 2009.
- [19] R. Rai, A. De, H. K. D. H. Bhadeshia and T. DebRoy, "Review: friction stir welding tools," *Science and Technology of Welding and Joining 2011 VOL 16 NO 4 325*, vol. 16, no. 4, pp. 325-342, 2011.